International Global Navigation Satellite Systems Society
IGNSS Symposium 2011

University of New South Wales, Sydney, NSW, Australia
15 – 17 November 2011

A-RAIM vs. R-RAIM: A Comparative Study

Yiping Jiang (1)
The University of New South Wales/Australia
Yiping.jiang@student.unsw.edu.au
Jinling Wang (2)
The University of New South Wales/Australia
Jinling.wang@unsw.edu.au

ABSTRACT

GNSS Receiver Autonomous Integrity Monitoring (RAIM) has been widely used in civil aviation with the purpose of keeping the users notified of the integrity risk of the navigation solutions. It is based on the scheme of consistency check among redundant observations and therefore independent of any augmentation systems. With the modernized GPS and GLONASS, as well as the new GNSS systems (Compass, GALILEO) well underway, the increase in the number of satellites and the multiple frequency signals are available. It is therefore reasonable to pursue the possibility of using RAIM in civil aviation for more stringent procedures, such as LPV-200 for vertical guidance on a global scale. This possibility is explored by US Federal Aviation Administration (FAA) under the panel of GNSS Evolutionary Architecture Study (GEAS), which has attracted attention of researchers thereafter. Two major architectures have been identified as feasible choices to meet the LPV-200 requirement: a) Advanced RAIM (A-RAIM), b) Relative RAIM (R-RAIM). With different advantages and disadvantages for the two architectures, it is realistic to have a comprehensive comparison. And then, reasonable choices can be made based on the requirements for specific applications.

The comparison is conducted mainly at the algorithm level. In this paper, the Multiple Hypotheses Solution Separation (MHSS) method based on local tests with multiple alternative hypotheses is adopted. Based on the common threat model, A-RAIM and R-RAIM are compared with results of VPL. The comparison of VPL within a world-wide map and a time series is provided to illustrate the difference. This paper is concluded with analysis and suggestions based on the comparison.

KEYWORDS: RAIM, R-RAIM, A-RAIM, GNSS, Civil Aviation

1. INTRODUCTION

Currently, there are three technologies that can monitor integrity in GNSS based navigation for civil aviation including RAIM, Ground-based Augmentation System (GBAS) and Satellite-based Augmentation System (SBAS). The integrity monitoring task is designed in the aircraft receiver, ground station and satellites separately. The tendency in the near future is to put the integrity monitoring responsibility in the satellites themselves with dual frequency diversity, new constellation, build-in integrity function in the constellation, etc. To take advantage of the future GNSS system and augmentation systems, A-RAIM and R-RAIM are designed as the two most promising integrity monitoring architectures. The purpose is to provide the LPV-200 service world-wide in the near future (GEAS, 2008; GEAS, 2010). In the latest report (GEAS, 2010), A-RAIM is the preferred choice and R-RAIM is only used when A-RAIM is unavailable. To make the service available, the following requirements must be met: Vertical Protection Level (VPL), Effective Monitoring Threshold (EMT) and the vertical positioning accuracy (Acc_v). The algorithm to output VPL results is of major interest for comparison in this paper.

With the details of the error model defined in the GEAS reports, a common method is needed to compare these two RAIM architectures at the algorithm level. There are mainly two major RAIM methods available: the slope-based method (Brown and Chin, 1998) and the solution separation method (Brenner, 1995). The solution separation method was applied in R-RAIM with optimization (Lee, 2008; Lee and McLaughlin, 2008). The comparison of both A-RAIM and R-RAIM was provided in (Gratton *et al.*, 2010) under the slope-based method. In this paper, the Multiple Hypotheses Solution Separation (MHSS) method (Juan *et al.*, 2007) is adopted for comparison which is also designed with the solution separation method. Service availability results with the world-wide coverage under different error model parameters and constellations were simulated in GEAS (2010) with the MHSS method under two architectures. In this paper, predicted VPL results versus location and time are simulated and compared to further illustrate the differences between A-RAIM and R-RAIM.

The paper is organised as follows. First, the integrity monitoring architecture is described with three parts: the common architecture, the positioning method used in RAIM and the RAIM FDE method. The comparison of the difference in RAIM positioning method for A-RAIM and R-RAIM is provided. Then, the two algorithms are developed in detail with the threat model, error model and the MHSS method. The results VPL from A-RAIM and R-RAIM are compared based on the above algorithms and suggestions are provided as to which architecture is better for certain scenarios.

2. INTEGRITY MONITORING ARCHITECTURE

2.1 Common Architecture

Within the current integrity monitoring architecture designs, all the integrity information is centralized as the Integrity Support Message (ISM) which contains the error model (fault rate, error distribution etc.) information from all kinds of augmentation and monitoring systems that needs to be provided to the user within a maximum delay of time-to-alert (TTA). Together with the GNSS measurements as shown in Fig. 1, it is possible to output the integrity monitoring results as the indicator of service availability.

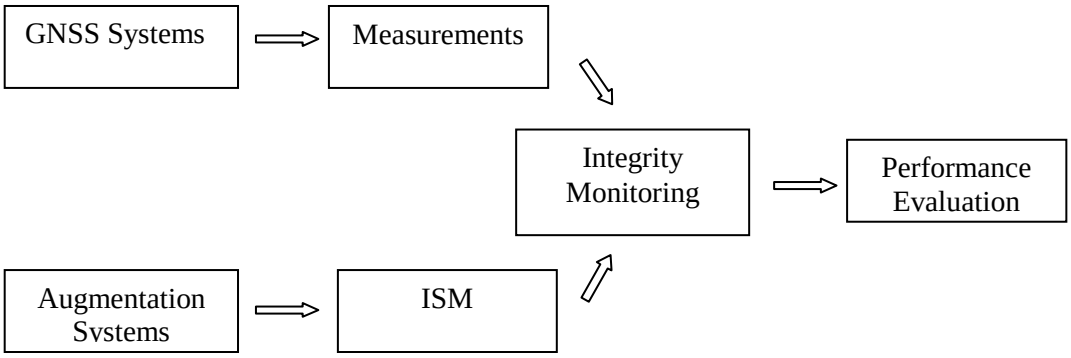

Figure 1. System State Diagram

2.2 Positioning Methods Used in RAIMs

2.2.1 A-RAIM Positioning Method

The normal snapshot positioning method is used for A-RAIM where position estimation is obtained using code measurements for the current time. Without any information from another time used, the estimation results are only influenced by current geometry and error model configurations.

2.2.2 R-RAIM Positioning Method

The positioning scenario for R-RAIM is shown in Fig. 2. Depending on the difference in merging two measurements, the initial one and the delta range, there are range domain and position domain methods. The range domain method merges these two types of ranges in the range domain and the position domain method merges them in the position domain. There are no obvious differences between these two different positioning methods with numerical results demonstrated in Ding and Wang (2011). The difference between these two methods for integrity monitoring is the different ways of error propagation. And this division does not exist for A-RAIM.

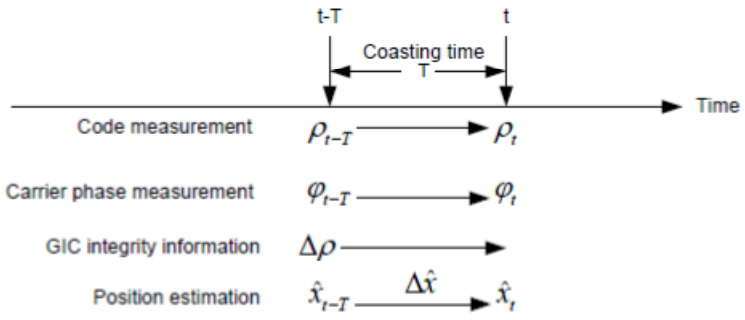

Figure 2. R-RAIM Positioning Method

2.2.3 Comparison for Positioning

Since the major difference between the two architectures is in the positioning method, a comparison is made as follows: 1) Only code measurements are used for A-RAIM, while both code and carrier phase measurements are used for R-RAIM; 2) In R-RAIM, delta-ranges are added to the initial position to obtain the current position, while in A-RAIM, the current position is obtained by current code measurements directly; 3) Taylor expansion can be used

for linearization for both methods, while a geometric relationship can also be used in R-RAIM for delta-range positioning (Van Graas 2005); 4) The sampling rate of position solution is decided by the sampling rate of raw measurements in A-RAIM, while the choice of coasting time is the factor that decides the sampling rate of the R-RAIM solution. 5) A-RAIM VPL is only a function of current time and location, while R-RAIM is related not only to current time and location but also to the initial time and location.

2.3 RAIM FDE methods

There is no difference between A-RAIM and R-RAIM for the Fault Detection and Exclusion (FDE) method. Depending on the choice of test statistic, there are also range domain and position domain method where the test statistic is in the range domain for the first method and position domain for the latter method. The popular RAIM method for the range domain method is the slope based method and the position domain method is the solution separation method (MHSS). The relationship between these two methods were derived in Blanch *et al*. (2007) leading to different integrity monitoring results as a results of different propagation from the test statistics domain to the position error domain. In this paper, for consideration of convenience, the position domain positioning and FDE methods are chosen as the MHSS method.

The differences between the slope based method and MHSS method include: 1) The MHSS method is based on a local test with multiple alternative hypotheses while the slope-based method is based on a global test statistic with single alternative hypotheses for fault detection purpose only. Consequently the test statistic from the first one is based on normal distribution and the latter one is Chi-square distribution. 2) The MHSS method is within the position domain with the test statistics defined as the difference between the all-in-view solution and the subset solution to produce results of the bound of position estimation error (Vertical Protection Level, VPL). The test statistics in the slope-based method is derived from the least squares residuals. 3) The worst case in the MHSS method is decided by the PL based on each alternative hypothesis while the worst case in the slope-based method is decided by the geometry which is the slope factor defined as the projection from the test statistics domain to the position domain.

The reasons for the adoption of the MHSS method includes: 1) It provides the flexibility in distribution of the total risk among different alternative hypotheses; 2) With the local test statistics, both the functionalities of fault detection and exclusion are included; 3) The algorithm is more straightforward in the position domain without any projection from other domains. While there are also disadvantages, e.g., the geometry screening is impossible with this method and the connection from the test statistics to positioning error is not clearly defined. They are regarded as less significant as compared with the advantages.

3. INTEGRITY MONITORING ALGORITHM

3.1 Threat Model

The threat model adopted here is consistent with the MHSS method where the integrity risk and continuity risk are defined based on the local test procedures. With the probability of fault mode H_j as P_{H_j} and the probability of any existence of harmful misleading information in the fault mode H_j as $P_{HMI|H_j}$, the total probability of the existence of any harmful misleading

information in the system is expressed as,

$$P_{HMI} = \sum_{j=0}^{M} P_{HMI|H_j} P_{H_j} \quad (1)$$

where M is the total number of fault modes. With H_0 as the fault free case, the follow condition is satisfied,

$$\sum_{j=0}^{M} P_{H_j} = 1 \quad (2)$$

The total number of fault modes is decided by the assumption of the type of faults that might exist in the GNSS system. With multiple constellations considered for future GNSS systems, it is necessary to include potential constellation faults besides satellite faults. The definition of a constellation fault is the fault that is consistent within one constellation while not consistent within multiple constellations, for example, the estimate of the earth orientation used for derivation of ephemeris parameters is faulty for an entire constellation.

With 2 constellations of K and J satellites each and each constellation independent with each other, if there is only single fault and single constellation fault, the total number of fault modes is,

$$M = K + J + 2 \quad (3)$$

If there are both single fault and double faults for both satellites and constellations,

$$M = K + J + 2 + C_K^2 + C_J^2 + C_2^2 \quad (4)$$

The continuity risk is designed with similar ideas. With the continuity risk defined based on fault mode H_j as $P_{cont|H_j}$, the total continuity risk is,

$$P_{cont} = \sum_{j=1}^{M} P_{cont|H_j} P_{H_j} \quad (5)$$

The probability of each fault mode is provided in GEAS (2010). With integrity risk and continuity risk defined based on each alternative hypothesis, it is possible to optimize the worst case by re-distribution of the total probability (Lee, 2008; Blanch, *et al.*, 2010).

3.2 Error Model

The error model for range measurements is comprised of a random component and a bias component with both characteristics carried in the ISM. Zero mean Gaussian distribution is assumed for the random part and therefore, it is the standard deviation that is in need. The standard deviation of the range error (clock and ephemeris) for evaluation of continuity and integrity purpose is used with the assumptions defined in GEAS (2008); GEAS (2010).

There are two types of bias magnitudes in the GEAS report for the error model. One is designed for the nominal condition b_{nom} used for evaluation of continuity in this paper. The other one is the maximum bias magnitude b_{max} used for evaluation of integrity. It should be noted here that this bias error is only assumed for integrity monitoring purpose, while it is not realistic to consider it for the FDE purpose.

3.3 A-RAIM based on MHSS

The functional model for positioning is expressed as,

$$y = Ax + \delta y \tag{6}$$

Where y is the observation vector with the covariance matrix as $\sigma^2 Q_y$, x is the user position vector, A is the design matrix obtained from linearization and δy is the error term.

The Least Squares estimation of the user position is,

$$\hat{x} = (A^T Q_y^{-1} A)^{-1} A^T Q_y^{-1} y \tag{7}$$

The position error is the difference between estimated and real position,

$$\tilde{x} = \hat{x} - x = S_0 \delta y \tag{8}$$

where $S_0 = (A^T Q_y^{-1} A)^{-1} A^T Q_y^{-1}$ is the projection matrix from observation error to position error.

Under the fault-free assumption H_0, the VPL is defined as,

$$VPL_0 = K_{md,0}\sigma_{v,0} + \sum_{j=1}^{M} |S_0|_{3,j} b_{max,j} \tag{9}$$

where $K_{md,0} = Q^{-1}(1 - \frac{1}{2}P_{HMI|H_0})$ and Q is the cumulative normal distribution, $\sigma_{v,0} = \sqrt{[cov(\tilde{x})]_{3.3}}$, $b_{max,j}$ is used to bound the worst case non-Gaussian errors for satellite j.

Under the fault mode H_j, the positioning error is separated into two parts,

$$\tilde{x} = \tilde{x}_j + \tilde{x}_{ss,j} \tag{10}$$

where the first part is $\tilde{x}_j = \hat{x}_j - x = S_j \delta y$ and $\hat{x}_j$ is the subset estimation with the jth observation excluded, $S_j = (A^T Q_j^{-1} A)^{-1} A^T Q_j^{-1}$ is the projection matrix from the observation to the subset estimation error, Q_j^{-1} is obtained by changing the jth row and column elements of Q_y^{-1} to zeros. The second part is $\tilde{x}_{ss,j} = \hat{x} - \hat{x}_j = (S_0 - S_j)\delta y$. The fault information is included in the positioning error $\tilde{x}_{ss,j}$ as in the method of solution separation.
The calculation of VPL is also separated into two parts. The first part is the bound for $\tilde{x}_j$. The integrity risk under this fault mode is used to bound the random error and the worst case non-Gaussian bias is used to bound the bias error.

$$D_{xj} = K_{md,j}\sigma_{v,j} + \sum_{j=1}^{M} |S_j|_{3,j} b_{max,j} \tag{11}$$

where $K_{md,j} = Q^{-1}(1 - \frac{1}{2}P_{HMI|H_j})$, $\sigma_{v,j} = \sqrt{[cov(\tilde{x}_j)]_{3.3}}$.

The second part is the bound for $\tilde{x}_{ss,j}$. The continuity risk is applied here for the random error and non-Gaussian error under the nominal case is used to bound the bias error.

$$D_{ss,j} = K_{fa,j}\sigma_{ss,j} + \sum_{j=1}^{M}\left|S_0 - S_j\right|_{3,j} b_{nom,j} \tag{12}$$

where $K_{fa,j} = Q^{-1}(1 - \frac{1}{2}P_{cont|H_j})$, $\sigma_{ss,j} = \sqrt{\left[cov(\tilde{x}_{ss,j})\right]_{3.3}}$ and $b_{nom,j}$ is used to bound the nominal case non-Gaussian errors under H_j.

Under the fault mode H_j, the VPL is defined as,

$$VPL_j = D_{xj} + D_{ss,j} \tag{13}$$

The final result of VPL is the maximum one among all fault modes,

$$VPL_{A-RAIM} = \max\{VPL_0, \max\{VPL_j\}\} \tag{14}$$

3.4 R-RAIM based on MHSS

The major difference between A-RAIM and R-RAIM is on the positioning part. There are two kinds of observation used at initial time and the delta time separately. The functional model for the initial time is,

$$y_0 = A_0 x_0 + \delta y_0 \tag{15}$$

where y_0 is the carrier phase smoothed code measurement vector at the initial time with SV Doppler effect adjustment (Van Graas 2005) and its covariance matrix as ${\sigma_0}^2 Q_0$.

The functional model for the delta time is,

$$y_\Delta = A_\Delta x_\Delta + \delta y_\Delta \tag{16}$$

Where y_Δ is relative carrier phase measurement vector with SV Doppler and change of geometry adjusted and its covariance matrix is ${\sigma_\Delta}^2 Q_\Delta$. For the relative range positioning, only satellites that are always available during this time period are used.

In R-RAIM, the relative carrier phase measurements are used for positioning of a relative range (Van Graas and Soloviev, 2005) which is added on the initial position using code measurements to obtain the current position estimation,

$$\hat{x} = \hat{x}_0 + \hat{x}_\Delta \tag{17}$$

where $\hat{x}_0$ is the initial position estimation and $\hat{x}_\Delta$ is the relative range estimation.

Therefore, the position error is,

$$\tilde{x} = \tilde{x}_0 + \tilde{x}_\Delta = R_0 \delta y_0 + R_\Delta \delta y_\Delta \tag{18}$$

where $R_0 = (A_0^T Q_0^{-1} A_0)^{-1} A_0^T Q_0^{-1}$ and $R_\Delta = (A_\Delta^T Q_\Delta^{-1} A_\Delta)^{-1} A_\Delta^T Q_\Delta^{-1}$.

Under the fault-free assumption H_0, the VPL is defined as,

$$VPL_0 = K_{md,0}\sigma_{v,0} + \sum_{j=1}^{M} |R_0 + R_\Delta|_{3,j} b_{max,j} \quad (19)$$

Since fault can only happen in the carrier phase measurement for relative positioning, with the code measurements for initial position estimation protected by GNSS Integrity Channel (GIC), only the relative position estimation error is divided into two parts under fault mode H_j,

$$\tilde{x}_\Delta = \tilde{x}_{\Delta,j} + \tilde{x}_{\Delta,ss,j} \quad (20)$$

where $\tilde{x}_{\Delta,j} = \hat{x}_{\Delta,j} - x_\Delta = R_{\Delta,j} y$ and $\hat{x}_{\Delta,j}$ is the subset estimation with the j[th] observation excluded. $\tilde{x}_{\Delta,ss,j} = \hat{x}_\Delta - \hat{x}_{\Delta,j} = \left(R_\Delta - R_{\Delta,j}\right) y$ and $\tilde{x}_{\Delta,ss,j}$ is defined with the idea of solution separation for fault detection.

As in the last section, the calculation of VPL is separated into two parts with the following term for the positioning error of $\tilde{x}_0 + \tilde{x}_{\Delta,j}$,

$$P_{xj} = K_{md,j}\sigma_{v,j} + \sum_{j=1}^{M} \left|R_0 + R_{\Delta,j}\right|_{3,j} b_{max,j} \quad (21)$$

where $K_{md,j} = Q^{-1}(1 - \frac{1}{2} P_{HMI|H_j})$, $\sigma_{v,j} = \sqrt{\left[cov(\tilde{x}_0 + \tilde{x}_{\Delta,j})\right]_{3.3}}$.

The second term is used to bound the error in $\tilde{x}_{\Delta,ss,j}$,

$$P_{ss,j} = K_{fa,j}\sigma_{ss,j} + \sum_{j=1}^{M} \left|R_\Delta - R_{\Delta,j}\right|_{3,j} b_{nom,j} \quad (22)$$

where $K_{fa,j} = Q^{-1}(1 - \frac{1}{2} P_{cont|H_j})$, $\sigma_{ss,i} = \sqrt{\left[cov(\tilde{x}_{\Delta,ss,j})\right]_{3.3}}$.

Under the fault mode H_j, the VPL is defined as,

$$VPL_j = P_{xj} + P_{ss,j} \quad (23)$$

The final VPL is,

$$VPL_{R-RAIM} = \max\left\{VPL_0, \max\left\{VPL_j\right\}\right\} \quad (24)$$

4. COMPARISON BY SIMULATION

4.1 VPL versus Location Results

With almanac information used, the predicted VPL is more conservative than the real time one where the simulated satellite position is used. The error model is the same as in (GEAS, 2008) with single fault assumed for both satellite and constellation. Predicted VPL results with world-wide distribution are shown in the following two figures with 25 GPS satellites.

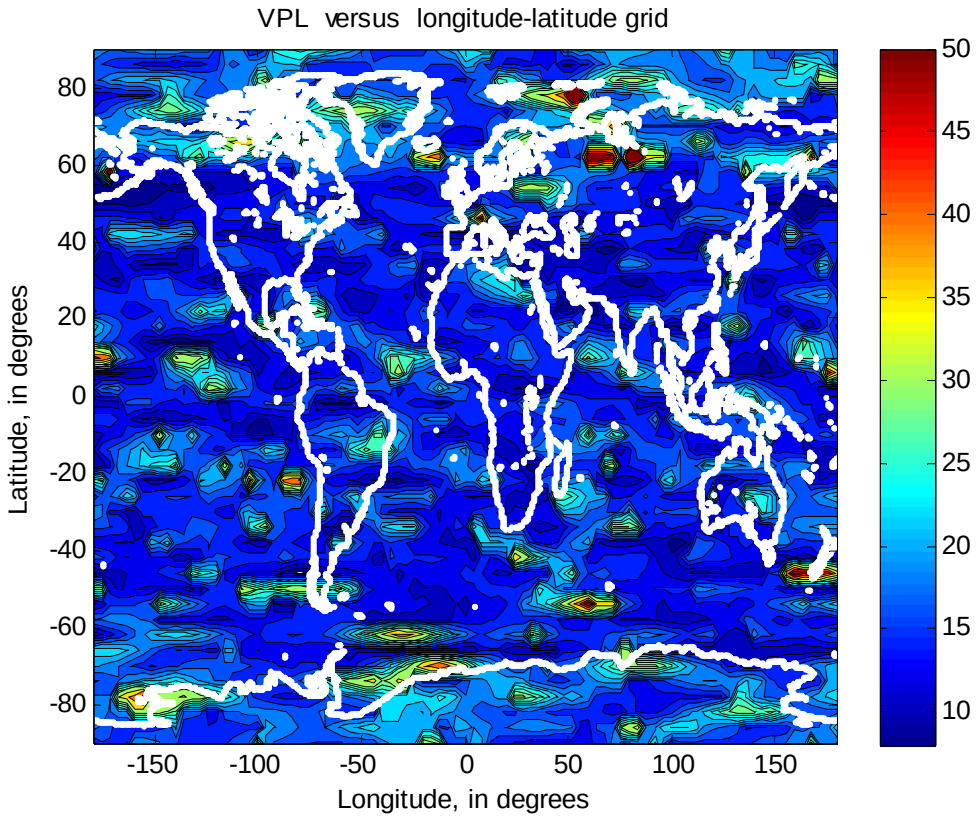

Fig. 3. A-RAIM, VPL versus location

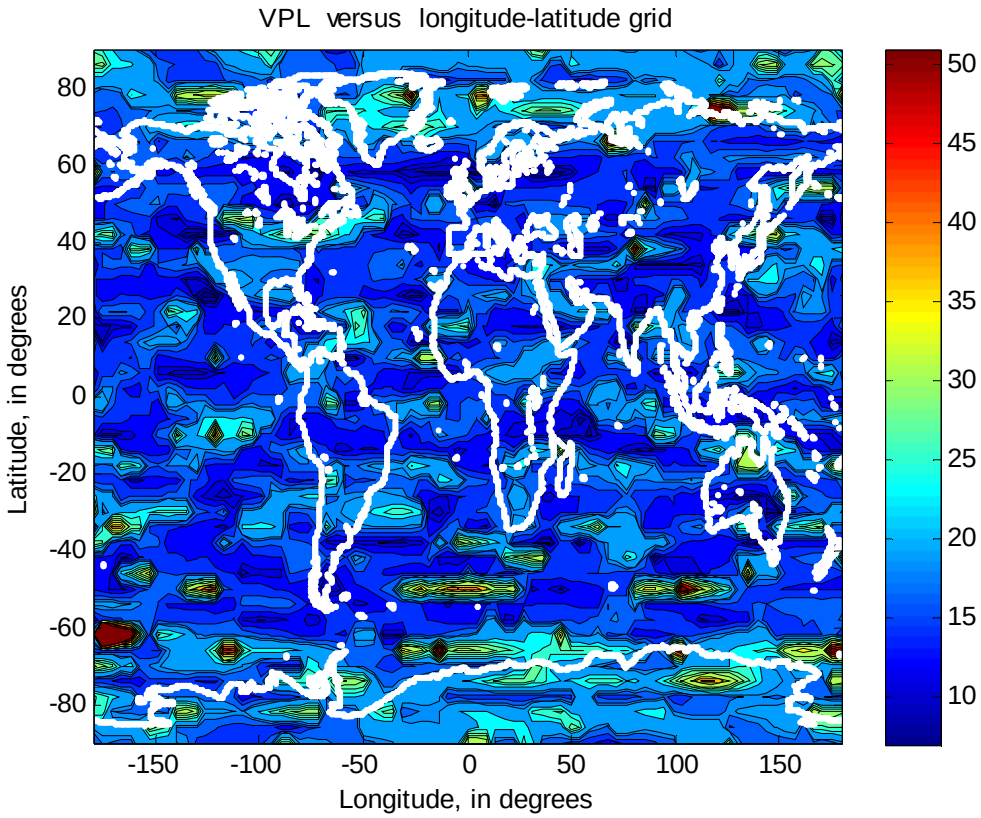

Fig.4. R-RAIM, VPL versus location

From the results of Fig. 3 and Fig. 4, R-RAIM has better results of VPL than A-RAIM

generally. This can be explained by the higher precision carrier phase measurements used in R-RAIM. Alert limit for LPV-200 is 35m which is compared with VPL to decide the service availability together with other factors. Based on this, the service availability of R-RAIM is higher than A-RAIM. But there are also exceptions at some locations where A-RAIM obtains better results than R-RAIM. It is mainly contributed by satellites lost during the coasting time in R-RAIM resulting in worse geometry and the higher precision is not enough to compensate this effect.

4.2 VPL versus Time

The VPL versus time results are used to show time dynamics' influence on the final results. The location is fixed at Sydney with 24hour time span.

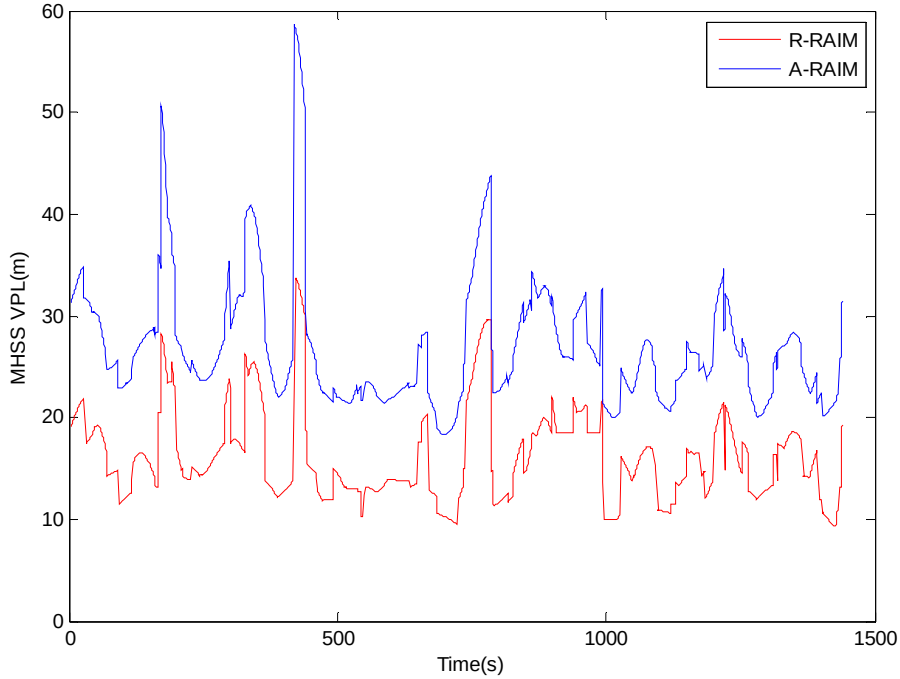

Fig. 5. A-RAIM and R-RAIM, VPL versus time

From Fig. 5, the results from R-RAIM are better than A-RAIM during the simulation time span. With geometry as the major influencing factors for the final results and related to time, results of A-RAIM is only related to current time while results of R-RAIM is related to both initial time and current time. The influence of time dynamics on R-RAIM is reflected by the difference in Fig. 5.

5. CONCLUSIONS

The two integrity monitoring architectures are illustrated in this paper under the MHSS method. The geometry is still a limiting factor to improve service availability for both architectures which will be much improved with more visible satellites in the near future. The major difference between these two methods is on the position estimation method which introduces different ways of error propagation for the concern of the integrity monitoring. The time and location dynamics are factors that can influence geometry, and therefore the results of VPL. The simulated results of R-RAIM VPL and A-RAIM VPL versus location and time

are provided with the conclusion that R-RAIM produces better results than A-RAIM in general.

The complexity of R-RAIM method also introduces some issues, such as the increased computation burden, the risk of any fault in the initial position, the choice of coasting time and the chance of lost satellite during the coasting time. The GIC information for the initial position estimation is trusted totally with no risk probability distributed here. If there is any fault in the initial measurement, the current design of R-RAIM is not able to protect the user from it. Also, the coasting time should be properly chosen since it can influence the probability of cycle slipe, satellite fault and the lost of satellites, the geometry change during this time and the parameters in the error model. All these factors introduce certain amount of uncertainty in R-RAIM, but if all the above factors are not significant for certain applications, R-RAIM should be a better choice. If any of these factors is critical, and at the same time A-RAIM is able to produce satisfactory results, A-RAIM should be used instead.

ACKNOWLEDGEMENTS

The first author is sponsored by the Chinese Scholarship Council for her PhD studies at the University of New South Wales, Australia.

REFERENCES

Blanch J, Ene A, Walter T and Enge P (2007) An Optimized Multiple Hypothesis RAIM Algorithm for Vertical Guidance, *ION GNSS 2007*, Fort Worth, TX.

Blanch J, Walter T, Enge P (2010) RAIM with Optimal Integrity and Continuity Allocations under Multiple Failures, *Aerospace and Electronic Systems, IEEE Transactions on*, 46(3):1235-1247

Brenner M. (1995) Integrated GPS/Inertial Fault Detection Availability, *Proceedings of the 8th International Technical Meeting of the Satellite Division of The Institute of Navigation (ION GPS 1995)*, Palm Springs, CA, 1949-1958.

Brown RG and Chin G (1998) GPS RAIM: Calculation of Threshold and Protection Radius Using Chi-Square Methods—A Geometric Approach, *Institute of Navigation Special Monograph Series*, Vol. V, Institute of Navigation, Alexandria, VA.

Ding W and Wang J (2011) Precise velocity estimation with a stand-alone GPS receiver, *Journal of Navigation, Royal Institute of Navigation*, 64(2), 1-15.

GEAS (2008) GNSS Evolutionary Architecture Study, *GEAS Phase I - Panel Report*, FAA.

GEAS (2010) GNSS Evolutionary Architecture Study, *GEAS Phase II - Panel Report*, FAA.

Gratton L, Mathieu J and Boris P (2010) Carrier Phase Relative RAIM Algorithms and Protection Level Derivation, *Journal of Navigation*, 63(2):215-231

Lee YC (2008) Optimization of Position Domain Relative RAIM, *ION GNSS 2008*, Savannah.

Lee YC and McLaughlin M (2008) A Position Domain Relative RAIM Method, *Proceedings of the IEEE/ION PLANS 2008 Conference*, Monterey, California.

Van Graas F and Soloviev A (2005) Precise Velocity Estimation Using a Stand-Alone GPS Receiver, *NAVIGATION*, 51(4):283-292